Rescue of the abnormal skeletal phenotype in Ts65Dn Down syndrome mice using genetic and therapeutic modulation of trisomic *Dyrk1a*

Joshua D. Blazek[1], Irushi Abeysekera[1], Jiliang Li[1], Randall J. Roper[1,*]

[1]Department of Biology, Indiana University-Purdue University Indianapolis and Indiana University Center for Regenerative Biology and Medicine, 723 W. Michigan Street, SL306, Indianapolis, IN 46202, USA.

[*]To whom correspondence should be addressed at: Department of Biology, Indiana University-Purdue University Indianapolis, 723 W. Michigan Street, SL 306, Indianapolis, IN 46202, Phone: (317) 274-8131, Fax: (317) 274-2846, Email: rjroper@iupui.edu

This is the author's manuscript of the article published in final edited form as:
Blazek, J. D., Abeysekera, I., Li, J., & Roper, R. J. (2015). Rescue of the abnormal skeletal phenotype in Ts65Dn Down syndrome mice using genetic and therapeutic modulation of trisomic Dyrk1a. Human molecular genetics, 24(20), 5687-5696. http://dx.doi.org/10.1093/hmg/ddv284

ABSTRACT

Trisomy 21 causes skeletal alterations in individuals with Down syndrome (DS) but the causative trisomic gene and a therapeutic approach to rescue these abnormalities are unknown. Individuals with DS display skeletal alterations including reduced bone mineral density, modified bone structure and distinctive facial features. Due to peripheral skeletal anomalies and extended longevity, individuals with DS are increasingly more susceptible to bone fractures. Understanding the genetic and developmental origins of DS skeletal abnormalities would facilitate the development of therapies to rescue these and other deficiencies associated with DS. *DYRK1A* is found in three copies in individuals with DS and Ts65Dn DS mice and has been hypothesized to be involved in many Trisomy 21 phenotypes including skeletal abnormalities. Return of *Dyrk1a* copy number to normal levels in Ts65Dn mice rescued the appendicular bone abnormalities, suggesting that appropriate levels of DYRK1A expression are critical for the development and maintenance of the DS appendicular skeleton. Therapy using the DYRK1A inhibitor EGCG improved Ts65Dn skeletal phenotypes. These outcomes suggest that the osteopenic phenotype associated with DS may be rescued postnatally by targeting trisomic *Dyrk1a*.

INTRODUCTION

Individuals with Down syndrome (DS) (OMIM 190685; ~1/700 live births (1)) display a multifaceted disorder with over 80 clinically defined phenotypes affecting nearly all organ systems (2). In addition to cognitive impairment, individuals with DS exhibit alterations in their appendicular skeletons, including an abnormal pattern of skeletal growth in the long bones during adolescence (3). Both children and adults with DS exhibit a reduction in bone mineral density (BMD) (4-6), an abnormal balance of bone formation and resorption during bone remodeling (7), which likely contribute to the high incidence of osteopenia and osteoporosis present in individuals with DS (8-11). Despite a gross structural understanding of the appendicular skeletal phenotypes, little is known about the genetic and cellular bases of altered bone development in individuals with DS.

The Ts(17^{16})65Dn (Ts65Dn) mouse, the most widely used DS model, contains a small marker chromosome that results in three copies of approximately half the gene orthologs found on human chromosome 21 (Hsa 21) (12). Ts65Dn mice exhibit numerous parallel phenotypes to humans with DS including cognitive, craniofacial, cardiac and bone abnormalities (13-16). Ts65Dn mice display a reduction in BMD, as well as osteoporotic-like structural deficiencies in the cortical and trabecular bone in adolescent and adult Ts65Dn skull and femurs (15, 17). It is hypothesized that deficiencies in osteoblast and osteoclast number and activity likely contribute to the Ts65Dn skeletal phenotype (18).

Despite the identification of structural bone abnormalities in humans with DS and Ts65Dn mice, little is known regarding how trisomic genes affect bone maintenance and homeostasis. *Dual-specificity tyrosine-(Y)-phosphorylation regulated kinase 1A* (*DYRK1A*) is found in three copies in humans with DS and Ts65Dn mice (19) and is hypothesized to be

involved in many DS phenotypes (20). Analysis of transgenic mice overexpressing *Dyrk1a* by 1.5 fold (theoretical dosage imbalance associated with trisomic genes in DS) identified severe appendicular skeletal deficiencies and an osteopenic phenotype similar to that observed in Ts65Dn mice (21). We hypothesize that increased *Dyrk1a* gene dosage and kinase activity results in the abnormal appendicular skeletal phenotype observed in adolescent Ts65Dn mice.

Parallel methodologies, one genetic and one therapeutic, were used to reduce DYRK1A activity to determine the contribution of *Dyrk1a* to the Ts65Dn appendicular skeletal phenotype. Ts65Dn mice were bred to *Dyrk1a*$^{+/-}$ heterozygote mutant mice to normalize the functional *Dyrk1a* gene copy number to euploid levels on an otherwise trisomic background. Ts65Dn mice were treated with a known DYRK1A inhibitor, Epigallocatechin-3-gallate (EGCG), which has been shown to decrease DYRK1A activity. We hypothesized that both the genetic and therapeutic rescue of DYRK1A activity would improve the abnormal Ts65Dn appendicular skeletal phenotypes.

RESULTS

Dyrk1a gene copy number affects bone density and structure in the Ts65Dn femur

The present data show that the femur in Ts65Dn DS mice exhibits a significantly lower bone mineral density (BMD) when compared to euploid mice (0.034 ± 0.002 vs. 0.043 ± 0.001; $p < 0.01$), confirming our previous conclusion that trisomy alters the normal mineralization of bone (15). The return of *Dyrk1a* to two functional copies in Ts65Dn mice (Ts65Dn, *Dyrk1a*$^{+/-}$) rescued the femoral BMD phenotype to euploid levels (0.041 ± 0.001). Though skull and mandible BMD were also lowered in Ts65Dn mice, these were not corrected in Ts65Dn, *Dyrk1a*$^{+/-}$ mice. Loss of 1 copy of *Dyrk1a* in euploid mice led to a significant decrease in mandible and skull BMD and a lowered femur BMD when compared to euploid animals (Supplemental Table 1), indicating that *Dyrk1a* copy number is important to normal bone growth and maintenance.

The microstructure of bone, as measured through microCT analyses, is also affected in Ts65Dn mice, as we have previously shown (15). Percent trabecular bone volume and trabecular thickness, number, and separation were rescued to euploid levels in the distal femur of Ts65Dn, *Dyrk1a*$^{+/-}$ mice (Fig. 1E-H). The 2D-cross sectional area of the cortical bone was similar between Ts65Dn, *Dyrk1a*$^{+/-}$ and euploid mice and significantly increased compared to Ts65Dn mice (Fig. 1I). No significant differences were observed on the 2D-cross sectional perimeter of the bone between Ts65Dn and Ts65Dn, *Dyrk1a*$^{+/-}$ mice (Fig. 1J). These data suggest that although the circumference of the periosteal surface in the femur midshaft is unchanged in Ts65Dn, *Dyrk1a*$^{+/-}$ as compared to Ts65Dn mice, the amount of bone material and overall thickness of the cortical bone is significantly improved to euploid levels in young adult mice.

***Dyrk1a* copy number impacts cell number and activity in the Ts65Dn femur**

Cells involved in bone modeling and remodeling are affected by *Dyrk1a* copy number. Histomorphometric analysis of the midshaft (cortical bone) and distal femur (trabecular bone) of 6 week old mice revealed significant alterations in cell number and activity in the Ts65Dn femur (Table 1). Mineral apposition rate (MAR), a measure of the rate at which osteoblasts are laying down new bone matrix, and bone formation rate (BFR), a measure of the total rate of new bone formation on the surface being mineralized, were significantly reduced in Ts65Dn cortical bone when compared to euploid animals. Cortical bone MAR and BFR was rescued in Ts65Dn, *Dyrk1a*$^{+/-}$ when compared to Ts65Dn mice (Table 1), suggesting increased *Dyrk1a* copy number leads to decreased periosteal mineralization in the Ts65Dn femur midshaft. Mineralization surface at the bone surface (MS/BS), a parameter estimating osteoblast number, was not significantly different in any of the four groups. Euploid, *Dyrk1a*$^{+/-}$ animals exhibited similar MS/BS, MAR, and BFR compared to euploid mice despite containing only one functional copy of *Dyrk1a.*

In the distal femur, the percent bone volume over total volume (BV/TV) is rescued to normal levels in Ts65Dn, *Dyrk1a*$^{+/-}$ mice (Table 1). Ts65Dn mice exhibit a significantly lower MS/BS, MAR, and BFR in the developing trabecular bone when compared to euploid mice and these differences were normalized in Ts65Dn, *Dyrk1a*$^{+/-}$ mice. Histological analysis of the bone cells in the distal femur identified a significant increase in osteoclast surface (OcS/BS), reflecting the percentage of bone surface covered by osteoclasts, and osteoclast number per mm bone surface (Oc#/mm BS) in Ts65Dn mice when compared to euploid mice and these values were rescued in Ts65Dn, *Dyrk1a*$^{+/-}$ animals. Despite lower MS/BS and MAR values, no difference was observed in osteoid surface/bone surface (OS/BS—representing the percentage of bone

surface where osteoblasts are laying down osteoid) in Ts65Dn mice when compared to euploid and Ts65Dn, *Dyrk1a*$^{+/-}$ animals (Table 1). Euploid, *Dyrk1a*$^{+/-}$ mice exhibited significantly lower MAR, BFR, and OS/BS, and significantly higher OcS/BS and Oc#/mm BS in the trabecular bone when compared to euploid and Ts65Dn, *Dyrk1a*$^{+/-}$ animals. No differences were observed in the trabecular bone parameters between Ts65Dn and euploid, *Dyrk1a*$^{+/-}$ mice except in MAR and OS/BS.

Mechanical Properties in Ts65Dn, *Dyrk1a*$^{+/-}$ Mice

Ts65Dn mouse femurs exhibit a significant decrease in ultimate force (general integrity of the bone), stiffness (related to the mineralization of the bone) and energy to failure (amount of energy required to break the bone), when compared to euploid mice (Fig. 2A-C). The force required to break the femur and stiffness were rescued to euploid levels in Ts65Dn, *Dyrk1a*$^{+/-}$ mice and energy to failure was increased when compared to Ts65Dn animals (Fig. 2A-C). Euploid, *Dyrk1a*$^{+/-}$ mice exhibit significant reductions in ultimate force and stiffness. These same mice have a lower energy to failure but this difference was not significant ($p = 0.07$). Assessment of the material properties of the femur, which take into account the overall size of the bone, revealed that Ts65Dn femurs exhibit a significantly lower toughness (amount of energy required to cause material failure; Fig. 2D) and normal ultimate stress and modulus (intrinsic strength and stiffness, respectively; Fig. 2E,F) when compared to euploid mice. Toughness is rescued to euploid levels in Ts65Dn, *Dyrk1a*$^{+/-}$ femurs (Fig. 2D).

Ts65Dn, *Dyrk1a*$^{+/-}$ Mice Exhibit Normalized Expression of *Dyrk1a* in the Femur

Analysis of RNA isolated from the femur of 6 week old Ts65Dn mice identified a 1.59 fold expression ($p = 0.15$) of *Dykr1a* RNA transcripts when compared to euploid mice. Ts65Dn, *Dyrk1a*$^{+/-}$ mice exhibited 1.01 fold *Dyrk1a* expression in the femur (compared to euploid) and this expression was not different from euploid levels ($p = 0.48$). The increased copy number of *Dyrk1a* in the Ts65Dn long bones also translated to DYRK1A kinase activity of 1.33 fold of that found in euploid animals ($p = 0.07$). Femurs from adolescent Ts65Dn, *Dyrk1a*$^{+/-}$ mice had 1.25 fold DYRK1A kinase activity when compared to euploid mice ($p = 0.13$).

Treatment with a DYRK1A inhibitor improves femoral BMD and trabecular microarchitecture in Ts65Dn mice

To determine if the known DYRK1A inhibitor EGCG (22) could improve the BMD and structural deficits observed in the Ts65Dn skeleton, we treated 3 week old Ts65Dn and euploid mice with EGCG (~9mg/kg/day) or water for 3 weeks. No differences were observed in the weight at 6 weeks of age, the amount of liquid consumed between Ts65Dn control and treated mice, or the dosage of EGCG received by Ts65Dn and euploid mice during the treatment period (Supplemental Fig. 1A-C). Ts65Dn mice treated with EGCG (Ts65Dn+EGCG) exhibited a significantly higher femoral BMD compared to Ts65Dn mice (0.038 ± 0.001 vs. 0.034 ± 0.001, $p < 0.05$), and similar to the genetic rescue, no effects were observed on mandible or skull BMD in Ts65Dn mice treated with postnatal EGCG (Supplemental Table 2). Treatment of euploid animals with EGCG did not have any effect on femur, skull, or mandible BMD (Supplemental Table 2).

EGCG treatment showed a positive impact on the Ts65Dn trabecular microarchitecture. Femurs from Ts65Dn+EGCG mice exhibited a significantly higher percent trabecular bone

volume, trabecular number, and trabecular thickness when compared to Ts65Dn mice (Fig. 3A, B, D), and were rescued to euploid levels. Additionally, treatment of euploid animals with EGCG did not have a significant impact on trabecular bone microarchitecture when compared to euploid animals (Fig. 3A-D). Unlike what was observed in trabecular bone, treatment with ~9 mg/kg/day EGCG for only 3 weeks did not correct the cortical bone phenotype observed in Ts65Dn mice (Fig. 3E,F).

EGCG treatment increases mineralization rate in Ts65Dn femurs with limited impact on strength

EGCG treatment of Ts65Dn mice led to a significant increase in mineral apposition rate (MAR) when compared to Ts65Dn mice but did not reach euploid levels in the cortical bone of the midshaft (Table 2). Despite significantly increasing MAR, EGCG treatment did not significantly increase overall bone formation rate (BFR) in the cortical bone of Ts65Dn mice. EGCG treatment had no effect on MS/BS, MAR, or BFR in the midshaft of euploid animals. Treatment of Ts65Dn mice with ~9 mg/kg/day EGCG led to a normalization of BV/TV (Table 2). Treatment with EGCG for 3 weeks also increased mineralizing surface (MS/BS), mineral apposition rate (MAR), and bone formation rate (BFR) in the trabecular bone of the distal femur in Ts65Dn mice, but only MAR was returned to euploid levels (Table 2), suggesting that EGCG treatment positively effects osteoblast number and activity in the Ts65Dn distal femur. EGCG treatment also led to a significant decrease in osteoclast number and activity in the trabecular bone of Ts65Dn mice but these values were not completely rescued to euploid levels at the ~9mg/kg/day treatment level. Treatment of euploid mice with EGCG did not affect the mineralization properties or the cellular composition/activity in the distal femur. Ts65Dn mice treated with EGCG exhibited a significant increase in bone toughness when compared to Ts65Dn

mice suggesting that, similar to what was observed in Ts65Dn, *Dyrk1a*$^{+/-}$ mice, EGCG treatment positively impacted the material properties of the bone (Supplemental Table 3). Other mechanical and material properties of the bone were not improved in Ts65Dn mice with a 3 week, ~9mg/kg/day EGCG treatment. EGCG treatment did not significantly affect the mechanical properties of the euploid femur.

DYRK1A Activity in the Femur after Treatment with 9mg/kg/day EGCG

In Ts65Dn mice treated with water, DYRK1A kinase activity was 1.53 fold that of euploid controls ($p=0.24$) in protein isolated from 6 week old femurs. The DYRK1A kinase activity of Ts65Dn mice treated with ~9 mg/kg/day EGCG was 1.25 fold of euploid levels ($p = 0.33$).

DISCUSSION

Despite knowing that trisomy of human chromosome 21 causes DS, it is not clear how three copies of >300 genes affects the myriad phenotypes associated with the syndrome. Though it was once hypothesized that a single critical chromosomal region influenced all major Trisomy 21 phenotypes, mouse models and advanced molecular analyses point to an individual gene or a small group of genes that may be important in a single or multiple DS phenotypes (23, 24). Other experiments using mouse models of DS have confirmed this recent paradigm shift showing the impact of one or two trisomic genes on specific well-defined DS phenotypes (25-29). It has been hypothesized that trisomic *DYRK1A* contributes to the development of a number of DS phenotypes including cognitive impairment, Alzheimer's disease, and skeletal anomalies (20, 30, 31). Our results indicate that three copies of *Dyrk1a* are substantially responsible for the postnatal establishment and maintenance of the abnormal adolescent Ts65Dn appendicular bone phenotype. Percent bone volume, trabecular microarchitecture, bone toughness and distal femur mineralizing surface, mineral apposition rate, and osteoclast number are all rescued to euploid levels in Ts65Dn, *Dyrk1a*$^{+/-}$ mice suggesting that three copies of *Dyrk1a* is sufficient to cause the abnormal Ts65Dn femoral phenotype. Using the Ts65Dn mouse model, others have shown the importance of DYRK1A in cognitive and neurological phenotypes associated with DS (29).

The association of *Dyrk1a* with the establishment and maintenance of the abnormal adolescent Ts65Dn appendicular skeleton provides a potential therapeutic target to improve the abnormal bone phenotype in humans with DS. Preclinical trials in mouse models have indicated the efficacy of drug treatment to alleviate some behavioral and cognitive DS phenotypes in mice but most do not directly treat the product of a trisomic gene (32). Treatments containing EGCG

have been shown to improve some cognitive deficits in trisomic mouse models and humans with DS, using EGCG doses of ~100 mg/kg/day and ~9 mg/kg/day, respectively (30, 33). Our treatment of Ts65Dn mice for three weeks with the same concentration of EGCG used in human studies led to a substantial improvement in the postnatal femoral phenotype at 6 weeks of age. BMD, percent bone volume, and MAR were all significantly improved after EGCG treatment. Critical to the therapeutic potential of EGCG, only limited effects of treatment were observed in the bones of euploid mice. Our parallel genetic and therapeutic data, including a slight reduction in DYRK1A activity in the appendicular skeletal bones, suggest that EGCG treatment affects DYRK1A activity in Ts65Dn mice to alleviate some appendicular skeletal abnormalities.

Further research is necessary to determine the optimal dosage and timing of EGCG treatment of Ts65Dn mice to completely correct the abnormal skeleton. A higher dosage of or extended treatment with EGCG may be necessary to further reduce DYRK1A activity and correct cortical abnormalities. Yet, Euploid,*Dyrk1a*$^{+/-}$ mice show significantly reduced percent bone volume, trabecular thickness, 2D cross-sectional perimeter, and ultimate force and stiffness as compared to euploid control mice. These phenotypes are similar to those observed in Ts65Dn mice and indicate that both overexpression and inhibition of *Dyrk1a* may negatively impact bone homeostasis. Transgenic *Dyrk1a* overexpressing mice display neurological abnormalities as do *Dyrk1a*$^{+/-}$ mice (34, 35). DYRK1A overexpression and inhibition have both been shown to reduce *Rest* transcript levels that regulate pluripotency and cell fate in DS (36). Taken together, these studies indicate the importance of an optimal dosage of EGCG that leads to positive phenotypic changes in the abnormal DS skeleton and brain, while avoiding excessive inhibition of DYRK1A activity.

We have shown that increased *Dyrk1a* dosage does not affect the prenatal origins of the abnormal appendicular skeletal phenotype in mouse models of DS (37) but does affect the postnatal appendicular skeleton. This study has shown that increased *Dyrk1a* dosage also does not affect Ts65Dn mandibular or skull BMD, though the morphology has similarities to that seen in individuals with DS (14). Increased expression of other trisomic genes may cause small changes to the prenatal bone structure, and it is still unknown if increased dosage of *Dyrk1a* has a primary role in DS craniofacial morphology.

Analysis of the cellular composition and activity in trabecular bone revealed a mechanism that likely explains the osteopenic bone phenotype observed in Ts65Dn mice. Mineralizing surface, a parameter estimating osteoblast number, and MAR/BFR are significantly lower in the distal femur of Ts65Dn mice suggesting the bone formation is significantly affected by trisomy. No differences were observed in osteoid per bone surface, an alternative measure of osteoblast activity, but this discrepancy is likely because osteoid per bone surface is a static measure at a single time point where as mineralizing surface is a dynamic measure assessing the process of bone formation over a 7 day time period. Furthermore, Ts65Dn mice exhibited a significant increase in the number of osteoclasts in the secondary spongiosa of the adolescent distal femur, contrary to what has been previously described in the adult Ts65Dn appendicular skeleton (18). It is hypothesized that the differences observed between the studies likely result from the analysis of bone at different stages of maturity (6 weeks vs. 12 weeks) and suggests that DYRK1A may play a complex role in the regulation of osteoclast number in Ts65Dn mice during skeletal remodeling. Overall, the increased osteoclast number along with the reduction in osteoblast number and activity suggests an inherent deficiency in the maintenance of balance

between bone resorption and bone formation in Ts65Dn mice leading to the osteopenic phenotype observed at 6 weeks of age.

The finding of decreased osteoclast number in the adolescent Ts65Dn distal femur suggests a novel mechanism for the role of *Dyrk1a* in the postnatal establishment and maintenance of bone. *DYRK1A* dosage affects cell fate and differentiation in neuronal precursors and embryonic stem cells (36, 38). It is known that DYRK1A is a negative regulator of the key pro-osteoclastic transcription factor NFATc and thus contrary to what was found, it was hypothesized that increased *Dyrk1a* expression in the Ts65Dn femur would lead to a decrease in osteoclastogenesis. Analyses of other targets of the multifunctional DYRK1A kinase suggest a number of interactions involving DYRK1A and proteins known to affect osteoclasts (39). Overexpression of *Dyrk1a* in the brain of hyperhomocysteinemic mice leads to a significant increase in the phosphorylation of Erk, Mek, and Akt (40). pAkt and pErk have both been shown to be positive regulators of osteoclastogenesis and bone resorptive activity suggesting an alternative pathway by which DYRK1A may regulate osteoclasts in the Ts65Dn adolescent skeleton (41-43). Alternatively, DYRK1A has been shown to directly phosphorylate cyclic AMP response element binding protein (CREB) a known positive regulator of osteoclast differentiation and function (44, 45).

In addition to osteoclast homeostasis, angiogenesis is a critical component of bone development and growth. Trisomy 21 attenuates angiogenesis through endostatin (a potent anti-angiogenic molecule), and trisomic RCAN1 was found to suppress VEGFA (46). Anti-angiogenesis or inhibition of VEGF would suppresses bone formation and the enhancement of angiogenesis or activation of VEGF would stimulate bone formation. This suggests that a decrease in bone formation in DS may be caused by the attenuation of angiogenesis. It is still not

clear whether angiogenesis may play a role in bone homeostasis in the DS model. However, previous studies demonstrate EGCG suppresses angiogenesis by inhibiting the activation of HIF-1 and VEGF expression (47). In our study, the improvement in bone volume by EGCG likely occurred via mechanisms which are not related to angiogenesis.

Though our results suggest that *Dyrk1a* is associated with many of the abnormal skeletal phenotypes associated with DS, not all parameters were corrected in Ts65Dn, *Dyrk1a*$^{+/-}$ mice as differences in cortical bone perimeter did not reach euploid levels. Dyrk1a RNA levels and DYRK1A kinase activity were not completely reduced to euploid levels in the long bones of Ts65Dn, *Dyrk1a*$^{+/-}$ mice. These results suggest that RNA expression and DYRK1A activity are variable at a given time point and that other genes found in three copies in Ts65Dn mice having a role in bone maintenance or cortical bone differences could be affecting the appendicular bone phenotype. Treatment with ~9 mg/kg/day EGCG did not significantly lower the DYRK1A activity level similar to that found in Ts65Dn, *Dyrk1a*$^{+/-}$ mice. This measurement was at a static time point and may not have reflected the total decreased DYRK1A activity. It may be that the cumulative changes in DYRK1A activity over the 3 week treatment period were enough to normalize some bone parameters and a higher concentration or longer treatment of EGCG will be needed to normalize all bone parameters and DYRK1A activity. Alternatively, a lower EGCG dose may positively affect skeletal phenotypes including those that were not corrected with the present EGCG treatment. EGCG likely affects other proteins and cellular activities beyond those associated with DYRK1A. EGCG has been shown to have antioxidant activities that improve bone precursors (48) as well as an effect on matrix metalloproteinases that decrease osteoclast formation and differentiation *in vitro* (49). It is entirely possible that EGCG is affecting these and other mechanisms in the Ts65Dn mouse model to correct appendicular skeletal

abnormalities. However, the limited changes in euploid mice given EGCG suggest that EGCG affects *Dyrk1a* or other trisomic genes in the Ts65Dn mouse model.

We have identified increased *Dyrk1a* gene dosage as a major contributing factor to the abnormal appendicular skeletal phenotype observed in adolescent Ts65Dn mice. Mechanistically, increased osteoclast number and a decrease in osteoblast number and activity cause a severe imbalance between bone resorption and formation leading to the osteopenic phenotype observed in Ts65Dn mice. Further research must be conducted to identify the method in which *Dyrk1a* copy number affects signaling pathways critical to osteoclast and osteoblast differentiation and activity to determine how trisomy for *Dyrk1a* causes the altered cellular phenotype observed in the Ts65Dn femur. Postnatal treatment of Ts65Dn mice with EGCG, a known inhibitor to DYRK1A, shows promising results as a therapeutic treatment for the abnormal DS bone phenotype. Further research will focus on extending the treatment of Ts65Dn mice with EGCG for longer periods of time, as well as potentially identifying **an additional**, but still non-toxic, concentration of EGCG to maximize the positive effects of this therapy on bone development.

MATERIALS AND METHODS

Animals

Female B6EiC3Sn a/A-Ts(17^{16})65Dn (Ts65Dn) mice were purchased from the Jackson Laboratory (Bar Harbor, ME). $B6C3F_1$ mice were bred by crossing B6 females with C3H males. Ts65Dn males were generated at Indiana University-Purdue University Indianapolis (IUPUI) by crossing Ts65Dn females with $B6C3F_1$ males and identified by PCR genotyping (50). Ts65Dn (approximate 50% B6 and 50% C3H background with small marker [trisomic] chromosome) mothers generated the male mice used for the therapeutic treatment portion of this study. Only male mice were used due to the subfertile nature of Ts65Dn male mice and importance of Ts65Dn female mice in colony maintenance. Trisomic and euploid mice were aged to 3 weeks, at which point they were weaned from their mothers. At the time of weaning Ts65Dn and euploid mice were randomly assigned either water or 0.124 mg/ml EGCG for liquid consumption *ad libitum*. The mice were weighed and solutions were changed every other day for three weeks. Measurements of total liquid volume consumed were taken at the time of changing for the extent of the three week period and the total amount of liquid consumed was calculated over the span of treatment (Supplemental Fig. 1). For the reduction of *Dyrk1a* gene copy number experiment, *Dyrk1a* heterozygous mutant mice (*Dyrk1a*$^{+/-}$) were obtained from Dr. Mariona Arbones (Institut de Recerca Oncologica, Barcelona, Spain). *Dyrk1a*$^{+/-}$ mice were backcrossed to B6C3F1 mice for 7 generations to parallel the genetic background of Ts65Dn mice. Ts65Dn females were then bred to *Dyrk1a*$^{+/-}$ males to generate the four groups of mice used in the study (euploid, euploid, *Dyrk1a*$^{+/-}$ [only 1 functional copy of *Dyrk1a*], Ts65Dn, and Ts65Dn, *Dyrk1a*$^{+/-}$ [2 functional copies of *Dyrk1a*]). Mice were Ts65Dn genotyped as described above and *Dyrk1a* mice were genotyped as previously described (51). Male mice were weaned at 3 weeks of age and allowed

to age to 6 weeks. For both study groups, mice were injected IP at 5 weeks of age with 0.2 ml of 0.6% Calcein green dye diluted in saline solution, as well as four days later with 0.2 ml of 1.0% Alizarin red dye. Three days after the Alizarin red injection mice were euthanized and weighed. The femur, mandible, and skull were subsequently extracted and placed in 70% ethanol and stored at -20°C until further use. All animal use and protocols were approved by the IACUC committee at IUPUI School of Science and adhere to the requirements in the NIH Guide for the Care and Use of Laboratory Animals.

Protein Isolation, Immunoprecipitation, and Dyrk1a Kinase assay

Six week old mice were euthanized and femurs were extracted for protein (euploid [n=6], Ts65Dn [n=6], Ts65Dn, *Dyrk1a*$^{+/-}$ [n=3]; and euploid + water [n=5], Ts65Dn + water [n=6], Ts65Dn + EGCG [n=3]). The distal and proximal femur was removed and the marrow cavity flushed with 1x PBS prior to being snap frozen in liquid nitrogen. Bones were ground into a powder in a mortar and pestle with liquid nitrogen and placed into RIPA buffer with 1x protease cocktail inhibitor (Roche, Indianapolis, IN). Samples were then homogenized using a portable rotary grinder, incubated at 4°C, and centrifuged at 10,000 rpm for ten minutes. Protein concentration was analyzed using a Bradford assay. A total of 300 ug protein was cleared of extraneous antibodies, incubated with mouse anti-DYRK1A antibody (7D10, Abnova, Taipei, Taiwan), and immobilized with protein-G sepharose beads overnight. The beads were washed and subjected to a protein kinase assay as previously described (33, 52). Briefly, beads were incubated with kinase buffer solution (1 x kinase buffer, 200uM Dyrktide, 100 uM ATP, and [γ-^{32}P]ATP (2 μCi/sample). At the same time, 2 uM harmine (a strong inhibitor of DYRK1A activity) was added to some samples and used as a control to ensure proper detection of

DYRK1A activity. Samples were incubated for 50 minutes at 30°C and the reaction was stopped with 1/3 vol 100mM EDTA. 10 uL of each sample was blotted onto P81 paper (samples done in triplicate) and washed extensively with 5% phosphoric acid. Counts were made in a Beckman Liquid Scintillation counter. Relative kinase activity was determined by subtracting background activity from untreated and EGCG treated euploid and trisomic samples. Comparisons were made using euploid values as the standard.

RNA Isolation and qPCR

RNA was isolated from the 6-week old femur of euploid, Ts65Dn, and Ts65Dn. *Dyrk1a*$^{+/-}$ animals (n = 3 in each group) using the Trizol/chloroform method and cleared of extraneous DNA using DNAase as described in the RNA micro kit purchased from Invitrogen (Grand Island, NY). Briefly, femurs were extracted from mice, proximal and distal ends were removed, and the marrow cavity was flushed with 1x PBS. Femurs were snap frozen in liquid nitrogen and kept at -80°C until processing. Femurs were ground in liquid nitrogen using a sterile mortar and pestle, placed in Trizol, and further homogenized using a tissue rotary homogenizer. Chloroform was added to each sample to induce phase separation, and RNA was eluted from the aqueous phase using isopropanol. A total of 500ng RNA was converted to cDNA using Taqman reverse transcription reagents and quantitative PCR (qPCR) was performed using *Dyrk1a* (Target; Mm01209880_m1 and Mm00432929_m1 covering Dyrk1a exons 4-5 and 5-6, respectively, [NCBI Reference sequence NM_001113389.1], which correspond to exons 6-7 and 7-8 in the Dyrk1a genomic sequence depicted in Fotaki et al. 2002) and *Actb* (control; Mm00607939_s1) primers (Life Technologies) using the manufacturer's instructions (TaqMan Gene Expression Assay, Applied Biosystems, Foster City, CA). The crossing point (Cp) values (done in triplicate) from each target primer were analyzed and normalized to the reference probe

using the Applied Biosystems 7300 Real Time PCR System and software (53). Average values for each primer were compared between Ts65Dn and euploid as well as Ts65Dn, *Dyrk1a*$^{+/-}$ and euploid samples to compute expression fold changes.

Dual Energy X-ray Absorptiometry (DEXA)

The bone mineral content of the femur was analyzed using the Lunar Piximus DEXA machine (PIXImus Lunar Corp., Madison, WI). The machine was calibrated prior to each use. The femurs were placed caudal side down on the densitometer with ultrahigh resolution (0.18 mm x 0.18 mm) (54). Lunar Piximus 2 2.0 software was used to assess BMD, bone mineral content (BMC), and total bone area measurements.

μCT imaging and Analysis

Femurs were imaged using the Skyscan 1172 μCT machine at the Indiana University School of Medicine and analyzed using the CTrecon and CTan softaware from Skyscan as previously described (15). Briefly, femurs were thawed and placed in a Styrofoam mold fitted to the rotating stage in the machine. Bones were scanned, and the collection of images was reconstructed for analysis. 3D and 2D analysis were conducted on the trabecular and cortical bone, respectively, to obtain the parameters addressed in the study.

Tissue Processing and Histomorphometry

The left femur was separated at the midshaft and the proximal and distal femurs were processed, cut, and sectioned as previously described (15). One section per femur midshaft was read using a D-FL Epi-Fluorescence attachment on a Nikon Eclipse 80i DIC microscope.

Mineralizing surface (MS) was assessed by measuring the double label perimeter (dl.P), single label perimeter (sl.P), and total perimeter using BioQuant software (R & M Biometrics, Nashville, TN; MS = (dl.P. +1/2 sl.P)/Total perimeter). Mineral apposition rate (MAR) was determined by measuring the distance between the two fluorochrome labels, using Image J (National Institute of Health, Bethesda, MD), and averaging the distance by the days between label application (4). MS and MAR were used to calculate bone formation rate (BFR; BFR = MS*MAR*365 days/ year). These measures were made at the periosteal surface of the femur midshaft. For dynamic analysis of the distal femur, trabecular bone was thin sectioned (4μm) using a rotary microtome with a tungsten-carbide knife. Dynamic analysis was carried out using Bioquant software as mentioned above. For static histomorphometry of trabecular bone, 4 μm thin sections were deplasticized in acetone and stained for either osteoid using a modification of the Von Kossa/Macneal's (VKM) tetrachrome protocol (55) or osteoclasts using a tartrate-acid resistant acid phosphatase (TRAP) stain (56). Osteoid surface to bone surface (OS/BS) was quantified using Bioquant. For TRAP staining, osteoclast surface to bone surface and osteoclast number per 1mm tissue were quantified using Bioquant image analysis software.

Mechanical Testing

The mechanical strength of the femur was determined by 3-point bending (57) using a miniature materials machine at the Indiana University School of Medicine as previously described (15). Briefly, femurs were thawed, placed posterior side down on the 3-point bending apparatus with lower supports fixed at a distance of 7 mm apart and positioned in a manner so the force would be applied to the midpoint of the bone. The femur was preloaded using 0.1N to establish contact with the bone. The displacement rate was set at 0.1 mm/sec. Once preloaded,

force was applied until the bone was broken. Data was gathered by the system and Microsoft Excel was used to determine the ultimate load, energy to failure, and stiffness of the bone. Material properties were calculated as previously described (15).

Statistical Analysis

Data were analyzed in Microsoft Excel by comparing individual groups using a standard 2-tailed t-test and significance was denoted by p-values less than or equal to 0.05.

SUPPLEMENTARY MATERIAL

Table S1. Bone mineral density in Ts65Dn x *Dyrk1a* +/- offspring.

Table S2. Bone mineral density in Ts65Dn and euploid mice treated with EGCG or water.

Table S3. Effects of EGCG Treatment on the Mechanical and Material Properties of the Ts65Dn Femur.

Fig. S1. Weight and treatment consumption of Ts65Dn and euploid mice

ACKNOWLEDGMENTS

We thank Dr. Mariona Arbones for providing the *Dyrk1a*$^{+/-}$ mice and Dr. Matt Allen and Drew Brown for their help with mechanical testing and histomorphometric analysis. We are grateful to Danika Tumbleson for help with genotyping and Dr. Walter Becker and Dr. Steven Randall for aiding in the development and carrying out of the DYRK1A kinase assay, respectively. We thank Drs. Mariona Arbones, Grady Chism and Robert Yost for critical readings of the manuscript. This work was supported by grants from the Jerome Lejuene Foundation [R.J.R.];

the Blue River Community Foundation [R.J.R.]; a National Science Foundation GK-12 fellowship [grant number DGE 07042475 to J.D.B.] and the Purdue Research Foundation [J.D.B.].

Conflict of Interest statement: None declared.

REFERENCES

1 Parker, S.E., Mai, C.T., Canfield, M.A., Rickard, R., Wang, Y., Meyer, R.E., Anderson, P., Mason, C.A., Collins, J.S., Kirby, R.S. *et al.* (2010) Updated National Birth Prevalence estimates for selected birth defects in the United States, 2004-2006. *Birth Defects Res. A Clin. Mol. Teratol.*, **88**, 1008-1016.

2 Antonarakis, S.E. and Epstein, C.J. (2006) The challenge of Down syndrome. *Trends Mol. Med.*, **12**, 473-479.

3 de Moraes, M.E., Tanaka, J.L., de Moraes, L.C., Filho, E.M. and de Melo Castilho, J.C. (2008) Skeletal age of individuals with Down syndrome. *Spec. Care Dentist*, **28**, 101-106.

4 Guijarro, M., Valero, C., Paule, B., Gonzalez-Macias, J. and Riancho, J.A. (2008) Bone mass in young adults with Down syndrome. *Journal of intellectual disability research : JIDR*, **52**, 182-189.

5 Baptista, F., Varela, A. and Sardinha, L.B. (2005) Bone mineral mass in males and females with and without Down syndrome. *Osteoporos Int.*, **16**, 380-388.

6 Angelopoulou, N., Matziari, C., Tsimaras, V., Sakadamis, A., Souftas, V. and Mandroukas, K. (2000) Bone mineral density and muscle strength in young men with mental retardation (with and without Down syndrome). *Calcif. Tissue Int.*, **66**, 176-180.

7 McKelvey, K.D., Fowler, T.W., Akel, N.S., Kelsay, J.A., Gaddy, D., Wenger, G.R. and Suva, L.J. (2013) Low bone turnover and low bone density in a cohort of adults with Down syndrome. *Osteoporos Int.*, **24**, 1333-1338.

8 Center, J., Beange, H. and McElduff, A. (1998) People with mental retardation have an increased prevalence of osteoporosis: a population study. *American journal of mental retardation : AJMR*, **103**, 19-28.

9 Schrager, S. (2004) Osteoporosis in women with disabilities. *Journal of women's health*, **13**, 431-437.

10 van Allen, M.I., Fung, J. and Jurenka, S.B. (1999) Health care concerns and guidelines for adults with Down syndrome. *Am. J. Med. Genet.*, **89**, 100-110.

11 Carfi, A., Antocicco, M., Brandi, V., Cipriani, C., Fiore, F., Mascia, D., Settanni, S., Vetrano, D.L., Bernabei, R. and Onder, G. (2014) Characteristics of adults with down syndrome: prevalence of age-related conditions. *Frontiers in medicine*, **1**, 51.

12 Spellman, C., Ahmed, M.M., Dubach, D. and Gardiner, K.J. (2013) Expression of trisomic proteins in Down syndrome model systems. *Gene*, **512**, 219-225.

13 Moore, C.S. (2006) Postnatal lethality and cardiac anomalies in the Ts65Dn Down syndrome mouse model. *Mamm. Genome*, **17**, 1005-1012.

14 Richtsmeier, J.T., Baxter, L.L. and Reeves, R.H. (2000) Parallels of craniofacial maldevelopment in Down syndrome and Ts65Dn mice. *Dev. Dyn.*, **217**, 137-145.

15 Blazek, J.D., Gaddy, A., Meyer, R., Roper, R.J. and Li, J. (2011) Disruption of bone development and homeostasis by trisomy in Ts65Dn Down syndrome mice. *Bone*, **48**, 275-280.

16 Reeves, R.H., Irving, N.G., Moran, T.H., Wohn, A., Kitt, C., Sisodia, S.S., Schmidt, C., Bronson, R.T. and Davisson, M.T. (1995) A mouse model for Down syndrome exhibits learning and behaviour deficits. *Nat. Genet.*, **11**, 177-184.

17 Parsons, T., Ryan, T.M., Reeves, R.H. and Richtsmeier, J.T. (2007) Microstructure of trabecular bone in a mouse model for Down syndrome. *Anat. Rec. (Hoboken)*, **290**, 414-421.

18 Fowler, T.W., McKelvey, K.D., Akel, N.S., Vander Schilden, J., Bacon, A.W., Bracey, J.W., Sowder, T., Skinner, R.A., Swain, F.L., Hogue, W.R. *et al.* (2012) Low bone turnover and low BMD in Down syndrome: effect of intermittent PTH treatment. *PLoS One*, **7**, e42967.
19 Becker, W., Weber, Y., Wetzel, K., Eirmbter, K., Tejedor, F.J. and Joost, H.G. (1998) Sequence characteristics, subcellular localization, and substrate specificity of DYRK-related kinases, a novel family of dual specificity protein kinases. *The Journal of biological chemistry*, **273**, 25893-25902.
20 Arron, J.R., Winslow, M.M., Polleri, A., Chang, C.P., Wu, H., Gao, X., Neilson, J.R., Chen, L., Heit, J.J., Kim, S.K. *et al.* (2006) NFAT dysregulation by increased dosage of DSCR1 and DYRK1A on chromosome 21. *Nature*, **441**, 595-600.
21 Lee, Y., Ha, J., Kim, H.J., Kim, Y.S., Chang, E.J., Song, W.J. and Kim, H.H. (2009) Negative feedback Inhibition of NFATc1 by DYRK1A regulates bone homeostasis. *J. Biol. Chem.*, **284**, 33343-33351.
22 Bain, J., McLauchlan, H., Elliott, M. and Cohen, P. (2003) The specificities of protein kinase inhibitors: an update. *Biochem. J.*, **371**, 199-204.
23 Korbel, J.O., Tirosh-Wagner, T., Urban, A.E., Chen, X.N., Kasowski, M., Dai, L., Grubert, F., Erdman, C., Gao, M.C., Lange, K. *et al.* (2009) The genetic architecture of Down syndrome phenotypes revealed by high-resolution analysis of human segmental trisomies. *Proc. Natl. Acad. Sci. U S A*, **106**, 12031-12036.
24 Lyle, R., Bena, F., Gagos, S., Gehrig, C., Lopez, G., Schinzel, A., Lespinasse, J., Bottani, A., Dahoun, S., Taine, L. *et al.* (2009) Genotype-phenotype correlations in Down syndrome identified by array CGH in 30 cases of partial trisomy and partial monosomy chromosome 21. *Eur. J. Hum. Genet.*, **17**, 454-466.
25 Cataldo, A.M., Petanceska, S., Peterhoff, C.M., Terio, N.B., Epstein, C.J., Villar, A., Carlson, E.J., Staufenbiel, M. and Nixon, R.A. (2003) App gene dosage modulates endosomal abnormalities of Alzheimer's disease in a segmental trisomy 16 mouse model of down syndrome. *J. Neurosci.*, **23**, 6788-6792.
26 Chakrabarti, L., Best, T.K., Cramer, N.P., Carney, R.S., Isaac, J.T., Galdzicki, Z. and Haydar, T.F. (2010) Olig1 and Olig2 triplication causes developmental brain defects in Down syndrome. *Nat. Neurosci.*, **13**, 927-934.
27 Cooper, J.D., Salehi, A., Delcroix, J.D., Howe, C.L., Belichenko, P.V., Chua-Couzens, J., Kilbridge, J.F., Carlson, E.J., Epstein, C.J. and Mobley, W.C. (2001) Failed retrograde transport of NGF in a mouse model of Down's syndrome: reversal of cholinergic neurodegenerative phenotypes following NGF infusion. *Proc. Natl. Acad. Sci. U S A*, **98**, 10439-10444.
28 Hill, C.A., Sussan, T.E., Reeves, R.H. and Richtsmeier, J.T. (2009) Complex contributions of Ets2 to craniofacial and thymus phenotypes of trisomic "Down syndrome" mice. *Am. J. Med. Genet. A*, **149A**, 2158-2165.
29 Garcia-Cerro, S., Martinez, P., Vidal, V., Corrales, A., Florez, J., Vidal, R., Rueda, N., Arbones, M.L. and Martinez-Cue, C. (2014) Overexpression of Dyrk1A Is Implicated in Several Cognitive, Electrophysiological and Neuromorphological Alterations Found in a Mouse Model of Down Syndrome. *PLoS One*, **9**, e106572.
30 De la Torre, R., De Sola, S., Pons, M., Duchon, A., de Lagran, M.M., Farre, M., Fito, M., Benejam, B., Langohr, K., Rodriguez, J. *et al.* (2014) Epigallocatechin-3-gallate, a DYRK1A inhibitor, rescues cognitive deficits in Down syndrome mouse models and in humans. *Mol. Nutr. Food Res.*, **58**, 278-288.

31 Park, J. and Chung, K.C. (2013) New Perspectives of Dyrk1A Role in Neurogenesis and Neuropathologic Features of Down Syndrome. *Experimental neurobiology*, **22**, 244-248.
32 Gardiner, K.J. (2015) Pharmacological approaches to improving cognitive function in Down syndrome: current status and considerations. *Drug design, development and therapy*, **9**, 103-125.
33 Pons-Espinal, M., Martinez de Lagran, M. and Dierssen, M. (2013) Environmental enrichment rescues DYRK1A activity and hippocampal adult neurogenesis in TgDyrk1A. *Neurobiol. Dis.*, **60C**, 18-31.
34 Fotaki, V., Martinez De Lagran, M., Estivill, X., Arbones, M. and Dierssen, M. (2004) Haploinsufficiency of Dyrk1A in mice leads to specific alterations in the development and regulation of motor activity. *Behav. Neurosci.*, **118**, 815-821.
35 Martinez de Lagran, M., Altafaj, X., Gallego, X., Marti, E., Estivill, X., Sahun, I., Fillat, C. and Dierssen, M. (2004) Motor phenotypic alterations in TgDyrk1a transgenic mice implicate DYRK1A in Down syndrome motor dysfunction. *Neurobiol. Dis.*, **15**, 132-142.
36 Canzonetta, C., Mulligan, C., Deutsch, S., Ruf, S., O'Doherty, A., Lyle, R., Borel, C., Lin-Marq, N., Delom, F., Groet, J. *et al.* (2008) DYRK1A-dosage imbalance perturbs NRSF/REST levels, deregulating pluripotency and embryonic stem cell fate in Down syndrome. *Am. J. Hum. Genet.*, **83**, 388-400.
37 Blazek, J.D., Malik, A.M., Tischbein, M., Arbones, M.L., Moore, C.S. and Roper, R.J. (2015) Abnormal mineralization of the Ts65Dn Down syndrome mouse appendicular skeleton begins during embryonic development in a Dyrk1a-independent manner. *Mech. Dev.*, **136**, 133-142.
38 Hammerle, B., Ulin, E., Guimera, J., Becker, W., Guillemot, F. and Tejedor, F.J. (2011) Transient expression of Mnb/Dyrk1a couples cell cycle exit and differentiation of neuronal precursors by inducing p27KIP1 expression and suppressing NOTCH signaling. *Development*, **138**, 2543-2554.
39 Park, J., Song, W.J. and Chung, K.C. (2009) Function and regulation of Dyrk1A: towards understanding Down syndrome. *Cellular and molecular life sciences : CMLS*, **66**, 3235-3240.
40 Abekhoukh, S., Planque, C., Ripoll, C., Urbaniak, P., Paul, J.L., Delabar, J.M. and Janel, N. (2013) Dyrk1A, a serine/threonine kinase, is involved in ERK and Akt activation in the brain of hyperhomocysteinemic mice. *Molecular neurobiology*, **47**, 105-116.
41 Moon, J.B., Kim, J.H., Kim, K., Youn, B.U., Ko, A., Lee, S.Y. and Kim, N. (2012) Akt induces osteoclast differentiation through regulating the GSK3beta/NFATc1 signaling cascade. *Journal of immunology*, **188**, 163-169.
42 Neal, J.W. and Clipstone, N.A. (2001) Glycogen synthase kinase-3 inhibits the DNA binding activity of NFATc. *The Journal of biological chemistry*, **276**, 3666-3673.
43 He, Y., Staser, K., Rhodes, S.D., Liu, Y., Wu, X., Park, S.J., Yuan, J., Yang, X., Li, X., Jiang, L. *et al.* (2011) Erk1 positively regulates osteoclast differentiation and bone resorptive activity. *PloS One*, **6**, e24780.
44 Sato, K., Suematsu, A., Nakashima, T., Takemoto-Kimura, S., Aoki, K., Morishita, Y., Asahara, H., Ohya, K., Yamaguchi, A., Takai, T. *et al.* (2006) Regulation of osteoclast differentiation and function by the CaMK-CREB pathway. *Nature medicine*, **12**, 1410-1416.
45 Yang, E.J., Ahn, Y.S. and Chung, K.C. (2001) Protein kinase Dyrk1 activates cAMP response element-binding protein during neuronal differentiation in hippocampal progenitor cells. *J. Biol. Chem.*, **276**, 39819-39824.

46 Nizetic, D. and Groet, J. (2012) Tumorigenesis in Down's syndrome: big lessons from a small chromosome. *Nature reviews. Cancer*, **12**, 721-732.
47 Li, X., Feng, Y., Liu, J., Feng, X., Zhou, K. and Tang, X. (2013) Epigallocatechin-3-gallate inhibits IGF-I-stimulated lung cancer angiogenesis through downregulation of HIF-1alpha and VEGF expression. *Journal of nutrigenetics and nutrigenomics*, **6**, 169-178.
48 Yagi, H., Tan, J. and Tuan, R.S. (2013) Polyphenols suppress hydrogen peroxide-induced oxidative stress in human bone-marrow derived mesenchymal stem cells. *Journal of cellular biochemistry*, **114**, 1163-1173.
49 Oka, Y., Iwai, S., Amano, H., Irie, Y., Yatomi, K., Ryu, K., Yamada, S., Inagaki, K. and Oguchi, K. (2012) Tea polyphenols inhibit rat osteoclast formation and differentiation. *Journal of pharmacological sciences*, **118**, 55-64.
50 Reinholdt, L.G., Ding, Y., Gilbert, G.J., Czechanski, A., Solzak, J.P., Roper, R.J., Johnson, M.T., Donahue, L.R., Lutz, C. and Davisson, M.T. (2011) Molecular characterization of the translocation breakpoints in the Down syndrome mouse model Ts65Dn. *Mamm. Genome*, **22**, 685-691.
51 Fotaki, V., Dierssen, M., Alcantara, S., Martinez, S., Marti, E., Casas, C., Visa, J., Soriano, E., Estivill, X. and Arbones, M.L. (2002) Dyrk1A haploinsufficiency affects viability and causes developmental delay and abnormal brain morphology in mice. *Mo.l Cell. Biol.*, **22**, 6636-6647.
52 Papadopoulos, C., Arato, K., Lilienthal, E., Zerweck, J., Schutkowski, M., Chatain, N., Muller-Newen, G., Becker, W. and de la Luna, S. (2011) Splice variants of the dual specificity tyrosine phosphorylation-regulated kinase 4 (DYRK4) differ in their subcellular localization and catalytic activity. *J. Biol. Chem.*, **286**, 5494-5505.
53 Pfaffl, M.W. (2001) A new mathematical model for relative quantification in real-time RT-PCR. *Nucleic Acids Res.*, **29**, e45.
54 Li, J., Meyer, R., Duncan, R.L. and Turner, C.H. (2009) P2X7 nucleotide receptor plays an important role in callus remodeling during fracture repair. *Calcified tissue international*, **84**, 405-412.
55 Schenk, R., AJ OLAH and W Herrmann. (1984) Dickinson, G. (ed.), In *Methods of Calcified Tissue Peparation*. Elsevier, New York, pp. 1-56.
56 Erlebacher, A. and Derynck, R. (1996) Increased expression of TGF-beta 2 in osteoblasts results in an osteoporosis-like phenotype. *The Journal of cell biology*, **132**, 195-210.
57 Turner, C.H. and Burr, D.B. (1993) Basic biomechanical measurements of bone: a tutorial. *Bone*, **14**, 595-608.

LEGENDS TO FIGURES

Figure 1: Bone microstructure affected by *Dyrk1a* copy number. Trabecular structure differs between euploid (A), Ts65Dn (B), Ts65Dn, D*yrk1a*$^{+/-}$ (C), and euploid, *Dyrk1a*$^{+/-}$ (D) mice as revealed by microCT analyses. Ts65Dn, *Dyrk1a*$^{+/-}$ mice exhibit a euploid-like percent trabecular bone volume (E), trabecular number (F), separation (G), and thickness (H). Cortical bone analysis revealed a euploid-like 2D cross-sectional area (I) but not perimeter (J) in Ts65Dn, *Dyrk1a*$^{+/-}$ mice. Data are reported as mean ± SEM. Significance is denoted by brackets between groups ($p < 0.05$).

Figure 2: *Dyrk1a* copy number affects the mechanical properties of Ts65Dn bone. Ts65Dn mice exhibit significant reductions in ultimate force (A), stiffness (B), and energy to failure (C) when compared to Ts65Dn, *Dyrk1a*$^{+/-}$ and euploid mice. Quantification of the material properties of bone revealed significantly lower toughness (D) but normal ultimate stress (E) and modulus (F) in the Ts65Dn femur and toughness was rescued in the Ts65Dn, *Dyrk1a*$^{+/-}$ femur. Data reported as mean ± SEM; significance is denoted by brackets between groups ($p < 0.05$).

Figure 3: Comparison of femur parameters in EGCG treated and control mice. The distal femur of Ts65Dn and euploid mice treated with either EGCG or water were analyzed by MicroCT. Ts65Dn mice treated with EGCG exhibit significantly higher percent trabecular bone volume (A), trabecular number (B), no significant change in trabecular separation (C), and increased trabecular thickness (D) when compared to Ts65Dn untreated mice and are not significantly different from euploid mice. Treatment with EGCG had no effect on the area (E) or perimeter (F) in the cortical bone of the femur mid-shaft in adolescent Ts65Dn mice. EGCG treatment of euploid mice shows no differences from control euploid mice. Significance is denoted by brackets between groups ($p < 0.05$).

TABLES

Table 1. Histomorphometric Analysis of the Ts65Dn, *Dyrk1a*$^{+/-}$ Femur

	Euploid	Ts65Dn	Ts65Dn, *Dyrk1a*$^{+/-}$	Euploid, *Dyrk1a*$^{+/-}$
Cortical Bone				
MS/BS (%)	75.03 (4.47)	75.86 (4.12)	74.44 (3.99)	67.32 (4.39)
MAR (um/day)	4.18 (0.12)	3.37 (0.27) [A,B]	4.47 (0.26)	4.28 (0.34)
BFR (MAR*MS)	3.14 (0.17)	2.54 (0.23) [A,B]	3.37 (0.31)	2.91 (0.32)
Trabecular Bone				
BV/TV (%)	14.90 (0.70)	10.45 (0.55)[A,B,C]	13.33 (0.84)	13.06 (0.75)
MS/BS (%)	48.89 (1.83)	34.65 (2.14)[A,B]	48.73 (1.61)	40.11 (6.01)
MAR (um/day)	4.18 (0.11)	2.84 (0.20)[A,B,C]	4.22 (0.13)	3.51 (0.18)[A,B]
BFR (MAR*MS)	2.04 (0.10)	1.09 (0.10)[A,B]	2.06 (0.10)	1.42 (0.23)[A,B]
OS/BS (%)	18.33 (2.15)	18.08 (0.86)[B,C]	22.14 (1.59)	13.92 (1.53)[A,B]
OcS/BS (%)	7.30 (0.35)	10.23 (0.91)[A,B]	7.55 (0.30)	9.81 (0.98)[A,B]
Oc#/mm (n/mm)	3.17 (0.10)	3.88 (0.31)[A,B]	3.07 (0.14)	3.90 (0.33)[A,B]

MS/BS = mineralizing surface; MAR = mineral apposition rate; BFR = bone formation rate; BV/TV = percent bone volume for the entire femur; OS/BS = osteoid surface/bone surface; OcS/BS = osteoclast surface/bone surface; Oc#/BS = number of osteoclasts/1mm bone surface. [A] $p < 0.05$ when compared to euploid, [B] $p < 0.05$ when compared to Ts65Dn, *Dyrk1a*$^{+/-}$. [C] $p < 0.05$ when compared to euploid, *Dyrk1a*$^{+/-}$. Euploid (n=6), Ts65Dn (n=9), Ts65Dn, *Dyrk1a*$^{+/-}$ (n=8), Euploid, *Dyrk1a*$^{+/-}$ (n=7). Parameter values are listed as averages ± (SEM).

Table 2: EGCG affects the dynamic properties of the Ts65Dn femur

	Euploid	Ts65Dn	Ts65Dn +EGCG	Euploid + EGCG
Cortical Bone				
MS/BS (%)	71.49 (2.08)	71.50 (3.50)	76.44 (4.76)	72.69 (3.21)
MAR (um/day)	3.98 (0.23)	3.00 (0.18)[A,B,C]	3.41 (0.14)[A,C]	3.79 (0.16)
BFR (MAR*MS)	2.79 (0.15)	2.20 (0.21)[A,C]	2.61 (0.22)	2.75 (0.13)
Trabecular Bone				
BV/TV (%)	13.52 (0.87)	9.12 (1.09)[A,B,C]	12.60 (0.94)[C]	15.27 (0.62)[A]
MS/BS (%)	47.49 (1.47)	38.53 (2.08)[A]	43.18 (1.98)[A]	43.70 (1.68)
MAR (um/day)	3.56 (0.12)	2.95 (0.14)[A,B,C]	3.44 (0.15)	3.61 (0.14)
BFR (MAR*MS)	1.68 (0.04)	1.14 (0.09)[A,B,C]	1.49 (0.09)[A]	1.59 (0.08)
OS/BS (%)	17.36 (1.43)	18.06 (2.63)	21.67 (1.86)	17.17 (1.97)
OcS/BS)%)	6.84 (1.05)	10.87 (1.17)[A,B,C]	8.29 (0.67)[C]	6.33 (0.62)
Oc#/BS (n/mm)	2.61 (0.26)	4.40 (0.26)[A,C]	3.42 (0.29)[A,B.C]	2.52 (0.21)

MS/BS = mineralizing surface in the trabeculae; MAR = mineral apposition rate; BFR = bone formation rate; BV/TV = percent bone volume for the entire femur; Os/BS = osteoid surface/bone surface; OcS/BS = osteoclast surface/bone surface; Oc#/BS = number of osteoclasts/1mm bone surface. [A] $p < 0.05$ when compared to euploid, [B] $p < 0.05$ when compared to Ts65Dn + EGCG, [C] $p < 0.05$ when compared to euploid + EGCG. Euploid (n=8), Ts65Dn (n=7), Ts65Dn + EGCG (n=8), euploid + EGCG (n=9). Parameter values are listed as averages ± (SEM).

ABBREVIATIONS

Down syndrome (DS), bone mineral density (BMD), human chromosome 21 (Hsa 21), *Dual-specificity tyrosine-(Y)-phosphorylation regulated kinase 1A* (*DYRK1A*), Epigallocatechin-3-gallate (EGCG), Mineral apposition rate (MAR), bone formation rate (BFR), mineralization surface at the bone surface (MS/BS), percent bone volume over total volume (BV/TV), osteoclast surface (OcS/BS), osteoclast number per mm bone surface (Oc#/mm BS), osteoid surface/bone surface (OS/BS), and microcomputed tomography (μCT).

FIGURES

Figure 1

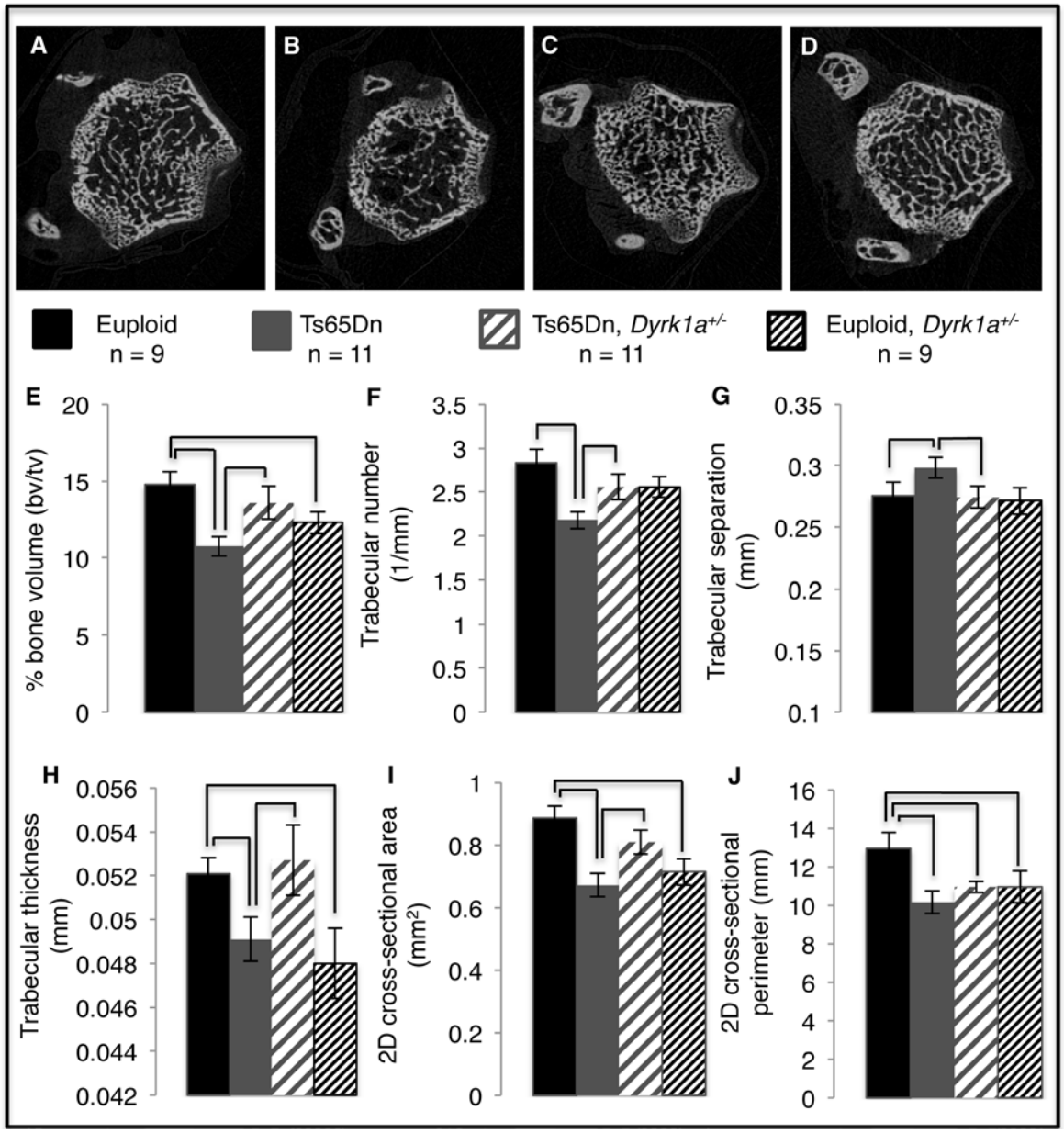

Figure 2

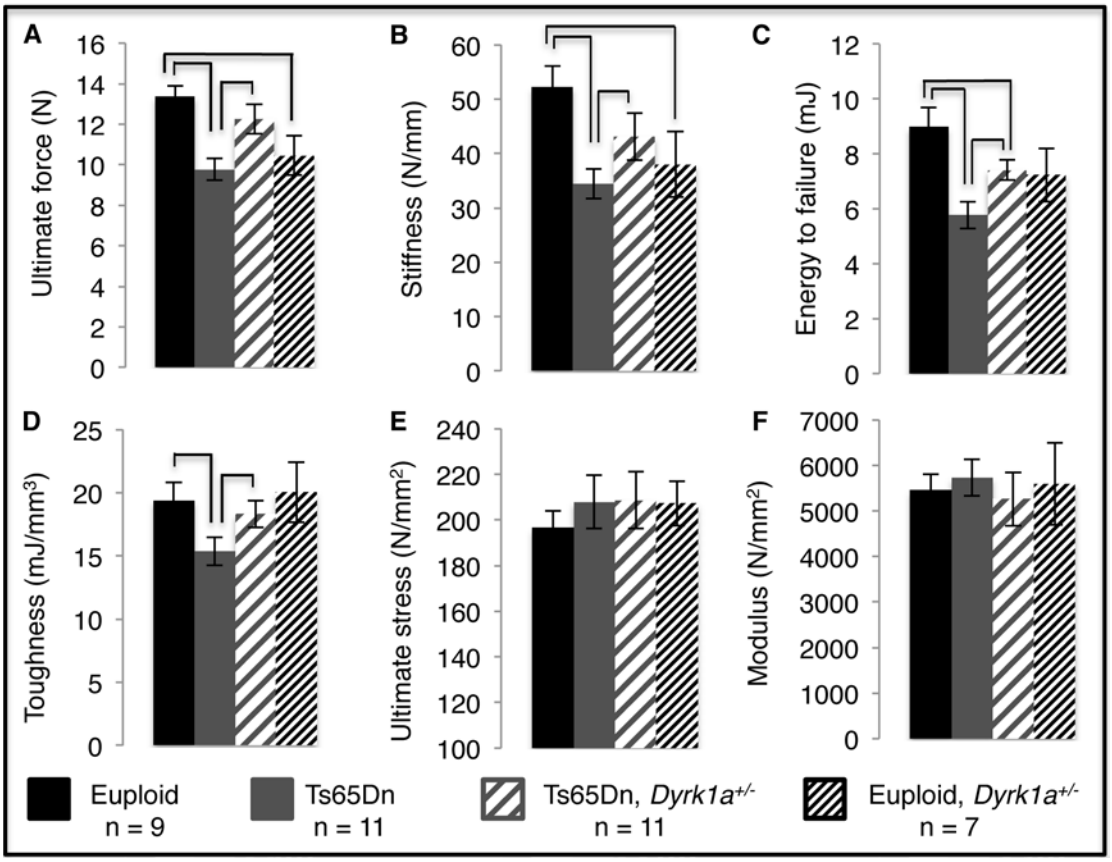

Figure 3

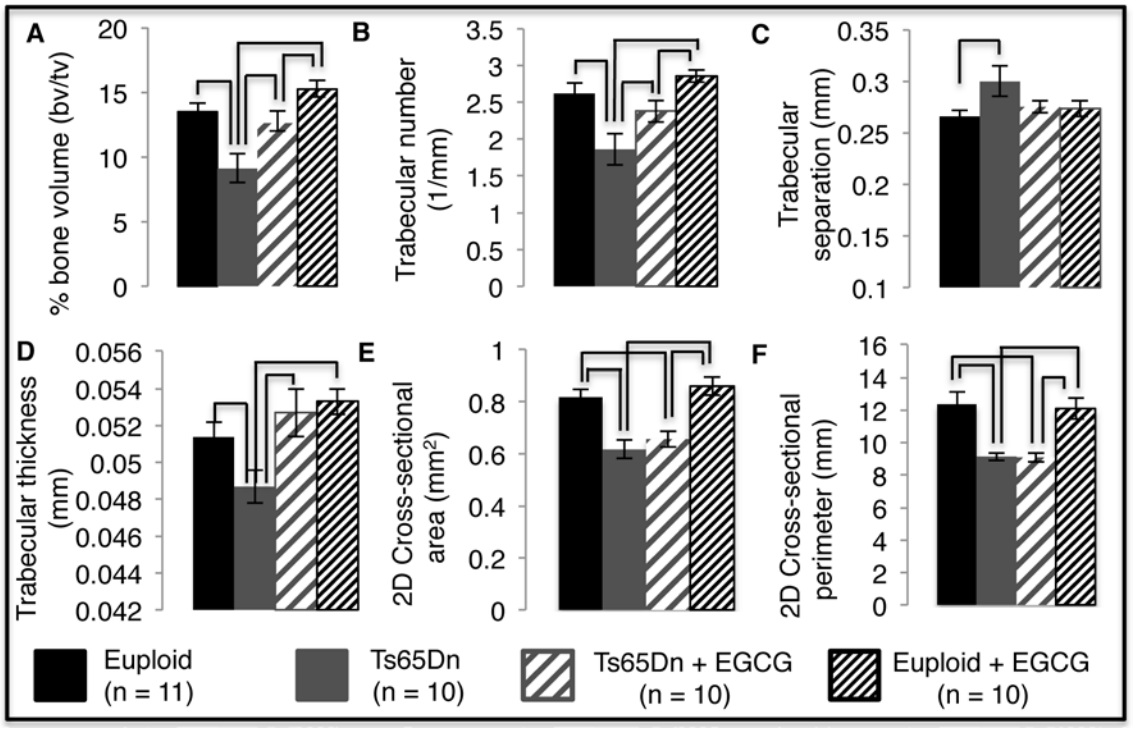

Supplemental Figure 1

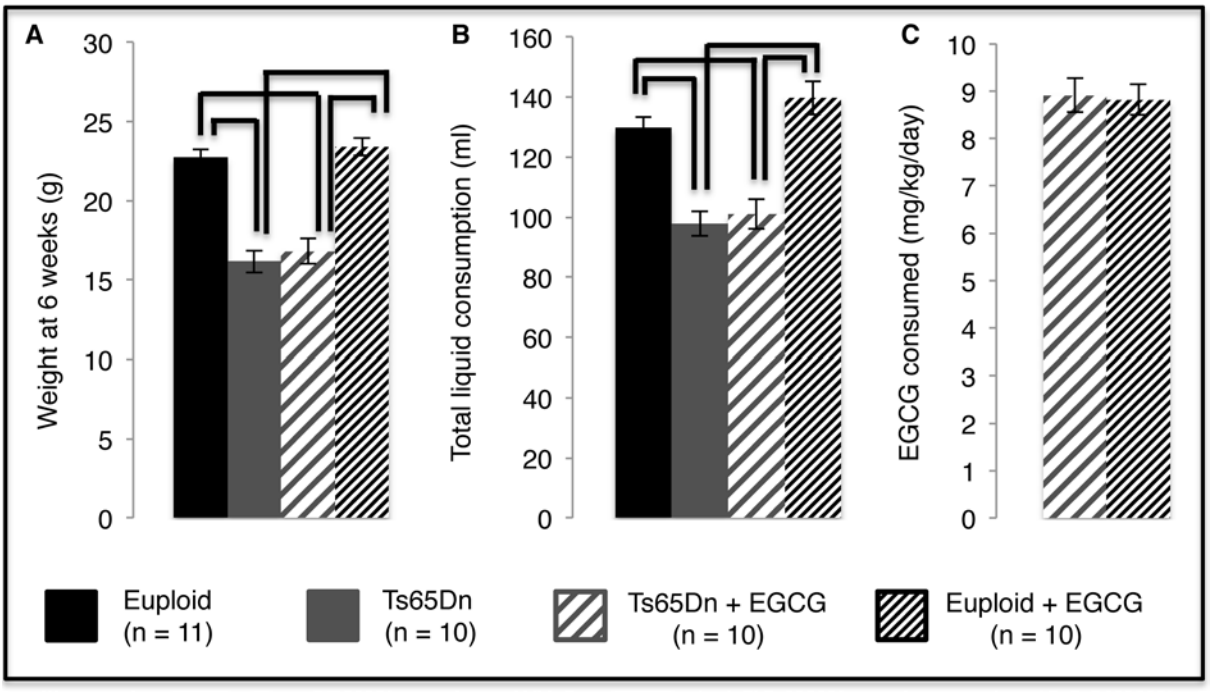

SUPPLEMENTAL INFORMATION

Supplemental Table 1: Bone mineral density in Ts65Dn x *Dyrk1a* +/- offspring.

	Euploid	Ts65Dn	Ts65Dn, *Dyrk1a*$^{+/-}$	Euploid, *Dyrk1a*$^{+/-}$
Femur	0.043 (0.001)	0.034 (0.002)^{A,B}	0.041 (0.001)	0.039 (0.002)
Skull	0.068 (0.009)	0.057 (0.001)^{A}	0.060 (0.002)^{A}	0.062 (0.001)^{A}
Mandible	0.080 (0.001)	0.072 (0.001)^{A,B}	0.076 (0.001)^{A}	0.074 (0.001)^{A}

^{A} $p < 0.01$ when compared to Euploid; ^{B} $p < 0.05$ when compared to Ts65Dn, *Dyrk1a*$^{+/-}$. Euploid (n=6), Ts65Dn (n=9), Ts65Dn, *Dyrk1a*$^{+/-}$ (n=8), Euploid, *Dyrk1a*$^{+/-}$ (n=7). Data are reported as mean ± (SEM).

Supplemental Table 2: Bone mineral density in Ts65Dn and Euploid mice treated with EGCG or water.

Supplemental Table 3: Effects of EGCG Treatment on the Mechanical and Material Properties of the Ts65Dn Femur.

	Euploid	Ts65Dn	Ts65Dn + EGCG	Euploid + EGCG
Femur	0.044 (0.002)	0.034 (0.001)^{A,B,C}	0.038 (0.002)^{,B,C}	0.045 (0.001)
Skull	0.067 (0.001)	0.059 (0.002)^{B,C}	0.059 (0.002)^{,B,C}	0.068 (0.001)
Mandible	0.081 (0.001)	0.072 (0.001)^{B,C}	0.073 (0.001)^{B,C}	0.080 (0.001)

^{A} $p < 0.05$ when compared to Ts65Dn+EGCG; ^{B} $p < 0.05$ when compared to Euploid; ^{C} $p < 0.05$ when compared to Euploid+EGCG. Euploid (n=8), Ts65Dn (n=7), Ts65Dn + EGCG (n=8), Euploid + EGCG (n=9). Data reported as mean ± (SEM)

	Euploid n = 10	Ts65Dn n = 8	Ts65Dn + EGCG n = 10	Euploid + EGCG n = 10
Ultimate Load (N)	13.77 (0.93)	9.61 (1.13)^{A}	10.93 (0.88)^{A}	14.68 (0.50)
Energy to Failure (mJ)	8.04 (0.71)	3.27 (0.54)^{A,B}	4.61 (0.34)^{A}	9.19 (0.79)
Stiffness (N/mm)	71.49 (5.40)	54.71 (7.08)^{A}	55.29 (4.88)^{A}	68.17 (6.26)
CSMI (mm^4)	0.094 (0.006)	0.065 (0.005)^{A}	0.072 (0.004)^{A}	0.102 (0.006)
Stress (N/mm^2)	198.28 (10.15)	178.34 (15.96)	185.26 (8.71)	199.07 (8.99)
Modulus (N/mm^2)	8247 (576)	9127 (956)	8197 (595)	7319 (742)
Toughness (mJ/m^3)	14.87 (1.49)	6.82 (1.02)^{A,B}	9.17 (0.84)^{A}	15.74 (1.30)

^{A} $p < 0.05$ when compared to Euploid; ^{B} $p < 0.05$ when compared to Ts65Dn + EGCG. Data reported as mean ± (SEM)

Supplemental Figure 1:

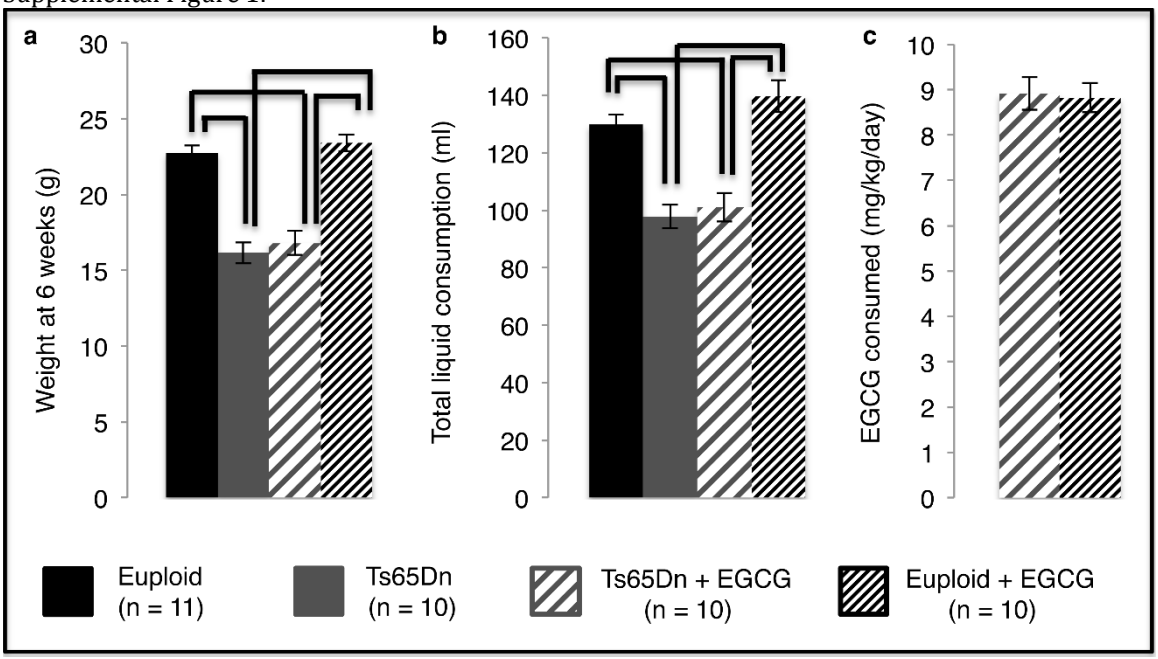

Supplemental Figure 1 Weight and treatment consumption of Ts65Dn and euploid mice. Ts65Dn and Ts65Dn + EGCG mice weighed the same on average at 6 weeks of age (a) and consumed the same amount of water or EGCG during the three week treatment period (b). Treated and untreated Ts65Dn mice consumed significantly less fluid and weighed significantly less at 6 weeks when compared to euploid and euploid treated mice. Ts65Dn + EGCG and Euploid + EGCG received a similar dosage of EGCG per day when body mass was taken into account (c). Brackets between groups denote a p-value < 0.05.